JOC Article

Photocyclization of Iminyl Radicals: Theoretical Study and Photochemical Aspects

Rafael Alonso, Pedro J. Campos, Miguel A. Rodríguez,* and Diego Sampedro*

Departamento de Química, Universidad de La Rioja, Grupo de Síntesis Química de La Rioja, Unidad Asociada al C.S.I.C., Madre de Dios, 51, 26006 Logroño, Spain

miguelangel.rodriguez@unirioja.es

Received November 30, 2007

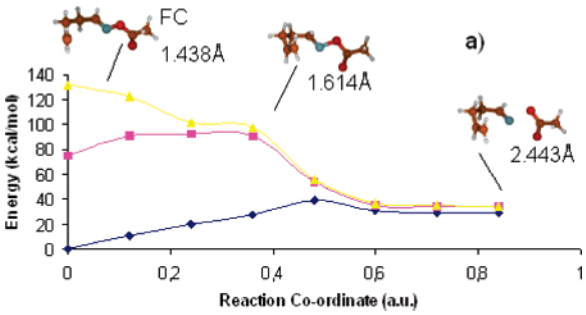

The irradiation of acyloximes was studied by theoretical methods. CASPT2/6-31G*//CASSCF/6-31G* calculations, using an active space of 14 electrons in 11 orbitals, indicate that S_2 should be the spectroscopic state, and its relaxation leads directly to N−O bond breakage due to coupling between the imine π^* and the σ^* N−O orbitals. Subsequent calculations at the B3PW91/6-31+G* level suggest that the resulting iminyl radicals are able to cyclize to the five- or six-membered ring, depending on the presence of a phenyl group as a spacer, a process that has been verified experimentally. The photochemical aspects of the more common five-membered ring formation, such as excited-state quenching, quantum yield, excited-state sensitizers, laser flash photolysis experiments, Stern−Volmer plot, and luminescence measurements, were investigated. These studies indicate that singlet and triplet excited states undergo the same reaction. Emission lifetimes of ca. $\tau = 10.6$ μs for compound **11** are suggestive of triplet parentage, while no fluorescence was detected, in agreement with the computed MEP energy profile.

Introduction

Iminyl radicals, generated by both thermal and photochemical methods, have proven to be valuable intermediates for the synthesis of five-membered nitrogen heterocyclic rings.[1−5] We recently described the synthesis of a range of isoquinoline derivatives through light-induced iminyl radical formation followed by addition to an unsaturated system (Scheme 1).[6] This capacity for linkage to generate either five- or six-membered rings prompted us to carry out an in depth study. Herein, we report a theoretical investigation and a photochemical study on the photocyclization of iminyl radicals generated by this method.

SCHEME 1

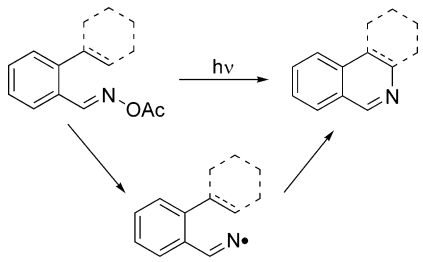

Computational Details

All reaction paths were computed using fully unconstrained ab initio quantum chemical computations in the framework of a

* Corresponding authors. Tel: +34-941299647. Fax: +34-941299621.

(1) For, a review see: Fallis, A. G.; Brinza, A. M. *Tetrahedron* **1997**, *53*, 17543.
(2) Gagosz, F.; Zard, S. *Synlett* **1999**, 1978.
(3) Uchiyama, K.; Hayashi, Y.; Narasaka, K. *Tetrahedron* **1999**, *55*, 8915.
(4) Mikami, T.; Narasaka, K. *Chem. Lett.* **2000**, 338.
(5) Kitamura, M.; Mori, Y.; Narasaka, K. *Tetrahedron Lett.* **2005**, *46*, 2373.
(6) Alonso, R.; Campos, P. J.; García, B.; Rodriguez, M. A. *Org. Lett.* **2006**, *8*, 3521.

10.1021/jo7025542 CCC: $40.75
Published on Web 02/22/2008

CASPT2//CASSCF strategy.[7] This requires the reaction coordinate to be computed at the complete active space self-consistent field (CASSCF) level of theory and the corresponding energy profile to be re-evaluated at the multiconfigurational second-order Møller-Plesset perturbation theory level (here we use the CASPT2 method implemented in MOLCAS-6.4)[8] to take into account the effect of electron dynamic correlation. The calculation of the reaction path was carried out using the 4-pentenal *O*-acyloxime **1** and the reaction coordinate was obtained via minimum energy path (MEP) computations at the CASSCF level with the 6-31G* basis set and an active space of 14 electrons in 11 orbitals (π and π^* orbitals of the imine, alkene, and carbonyl moieties, N and O lone pairs, and σ and σ^* orbitals for the N−O bond). The zeroth-order wave function used in the single-point CASPT2 calculations needed for the re-evaluation of the MEP energy profile (see above) is a three-root (S_0, S_1, S_2) state average CASSCF wave function. The same type of wave function was used where necessary in order to avoid convergence problems.

Radical ground-state calculations were carried out using the Gaussian 03 program package.[9] Becke's three-parameter hybrid exchange potential (B3)[10] was used with the Perdew−Wang (PW91)[11] gradient-corrected correlation functional, B3PW91. This method has been shown to describe bond cleavage more accurately than pure DFT methods.[12] The standard split-valence 6-31+G* basis set was employed. Geometry was fully optimized without any symmetry constraint for all model compounds. Optimized structures were characterized as minima or saddle points by frequency calculations, which also allowed ZPE and thermal corrections to be obtained.

Results and Discussion

Theoretical Calculations. In order to gain further insights into the reaction mechanism, we decided to explore this process by means of theoretical calculations. We tried to obtain a comprehensive view of the reaction path from light absorption to product formation. Thus, the level of theory used depended on the main process involved. The first part of the reaction mechanism involves a photochemically driven N−O cleavage and the CASPT2//CASSCF strategy was therefore used as this has proven to give reliable results for this kind of reaction.[7,13] In particular, we used model compound **1** to explore the photochemical reaction path using an active space of 14 electrons in 11 orbitals. We included π and π^* orbitals for the C=C, C=N and C=O double bonds, lone pairs for the nitrogen and oxygen atoms and the σ and σ^* orbitals for the N−O bond. The light absorption of model compound **1** was initially evaluated and the results are shown in Figure 1. The calculated n−π^* $S_0 \rightarrow S_1$ transition has an oscillator strength of 0.014 with a λ_{max} of 233 nm (123 kcal/mol, 5.32 eV), while the $\pi-\pi^*$ $S_0 \rightarrow S_2$ transition has an oscillator strength of 0.2 with a λ_{max} of 212 nm (135 kcal/mol, 5.86 eV). These values are consistent with the experimental spectrum of 5-hexen-2-one *O*-acetyloxime **2** (Figure 1), in which the bands appear at 234 nm with $f = 0.08$ and at 204 nm with $f = 0.23$. These data show that S_2 is the spectroscopic state while S_1 is an excited dark state. Excited-state relaxation was studied through an MEP calculation, as shown in Figure 2. Every step was obtained by minimization of the PES on a hypersphere centered on the initial geometry with a predefined radius at the CASSCF level (Figure 2a). Subsequent CASPT2 calculations were performed for the states of interest (S_0, S_1, and S_2) at each point of the MEP (Figure 2 b).

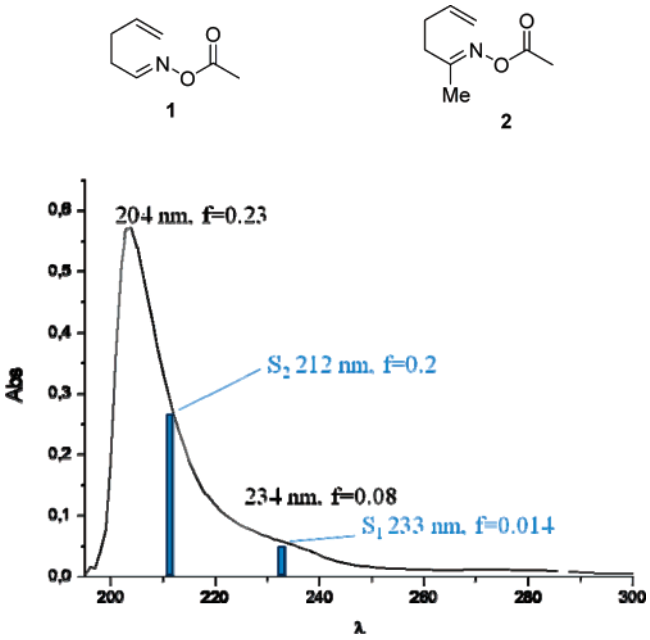

FIGURE 1. Calculated transitions (blue) for model **1** and experimental UV spectrum (black) for compound **2**.

As can be seen, relaxation on the S_2 PES leads directly to N−O bond cleavage. This is due to the coupling between the imine π^* and the σ^* N−O orbitals, which increases the occupancy of the σ^* orbital. Indeed, the first part of the MEP coordinate is controlled by N−O bond elongation, which leads to stabilization of the S_2 state and, as a consequence, to a decrease in the S_2-S_1 energy gap. The main geometry modification is the increase in the N−O bond length, while the rest of the molecule remains almost unchanged. Population of S_1 will be possible at this point given that the energy gap between S_1 and S_2 is small. Subsequent elongation of the N−O bond leads to further stabilization of S_1 (and S_2) and this in turn leads to a situation where two radicals are formed and the three PES become almost degenerate. The main geometric change in this part of the MEP corresponds with the two C−O distances which progressively become similar, as expected for the acetyl radical formation. The main features of the MEP are the same for both CASSCF and CASPT2 calculations. It should be noted, however, that the S_2/S_1 crossing takes place early after the

(7) Olivucci, M. *Computational Photochemistry*; Elsevier: Amsterdam 2005.
(8) Karlstrom, G.; Lindh, R.; Malmqvist, P.-A.; Roos, B. O.; Ryde, U.; Veryazov, V.; Widmark, P.-O.; Cossi, M.; Schimmelpfennig, B.; Neogrady, P.; Seijo, L. *Comp. Mater. Sci.* **2003**, *28*, 222.
(9) Gaussian 03, Revision C.02: Frisch, M. J.; Trucks, G. W.; Schlegel, H. B.; Scuseria, G. E.; Robb, M. A.; Cheeseman, J. R.; Montgomery, J. A.; Vreven, T.; Kudin, K. N.; Burant, J. C.; Millam, J. M.; Iyengar, S. S.; Tomasi, J.; Barone, V.; Mennucci, B.; Cossi, M.; Scalmani, G.; Rega, N.; Petersson, G. A.; Nakatsuji, H.; Hada, M.; Ehara, M.; Toyota, K.; Fukuda, R.; Hasegawa, J.; Ishida, M.; Nakajima, T.; Honda, Y.; Kitao, O.; Nakai, H.; Klene, M.; Li, X.; Knox, J. E.; Hratchian, H. P.; Cross, J. B.; Bakken, V.; Adamo, C.; Jaramillo, J.; Gomperts, R.; Stratmann, R. E.; Yazyev, O.; Austin, A. J.; Cammi, R.; Pomelli, C.; Ochterski, J. W.; Ayala, P. Y.; Morokuma, K.; Voth, G. A.; Salvador, P.; Dannenberg, J. J.; Zakrzewski, V. G.; Dapprich, S.; Daniels, A. D.; Strain, M. C.; Farkas, O.; Malick, D. K.; Rabuck, A. D.; Raghavachari, K.; Foresman, J. B.; Ortiz, J. V.; Cui, Q.; Baboul, A. G.; Clifford, S.; Cioslowski, J.; Stefanov, B. B.; Liu, G.; Liashenko, A.; Piskorz, P.; Komaromi, I.; Martin, R. L.; Fox, D. J.; Keith, T.; Al-Laham, M. A.; Peng, C. Y.; Nanayakkara, A.; Challacombe, M.; Gill, P. M. W.; Johnson, B.; Chen, W.; Wong, M. W.; Gonzalez, C.; Pople, J. A. Gaussian, Inc., Wallingford CT, 2004
(10) Becke, A. D. *J. Chem. Phys.* **1993**, *98*, 5648.
(11) Perdew, J. P.; Burke, K.; Wang, Y. *Phys. Rev. B* **1996**, *54*, 16533.
(12) Jensen, F. *Introduction to Computational Chemistry*; Wiley: New York, 1999; p 283.
(13) Kutateladze, A. G. *Computational Methods in Photochemistry*; CRC Press: Boca Raton, 2005.

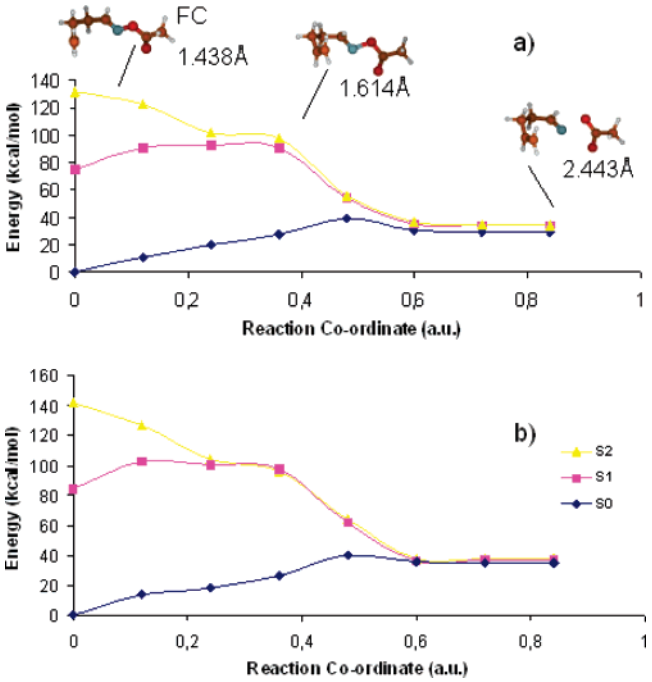

FIGURE 2. Evolution of the ground and two lowest singlet excited states for model **1** from the FC geometry along the S_2 MEP. Selected geometries are shown together with the N−O bond distance: (a) CASSCF, (b) CASPT2.

inclusion of electron correlation (Figure 2 b). These data clearly show that after irradiation the system readily undergoes a homolytic N−O bond cleavage to generate two radicals in the ground state: acetyl and iminyl radicals that can further react further. This easy bond cleavage is the reason behind the use of these kinds of systems as photoinitiators for UV-curable coatings.[14]

Once the iminyl radical reaches S_0, the remainder of the reaction path is controlled by ground state chemistry. In order to ensure this, we carried out a CASPT2 calculation of the iminyl radical to find out that the excited states (both S_1 and S_2) lie more than 70 kcal/mol above the ground state. Thus, the progress of the reaction, the regioselectivity and the effect of substituents were studied by means of DFT calculations. The choice of B3PW91 was made on the basis of previous results where this functional proved to give satisfactory results in radical chemistry.[15−19] After the photochemically induced homolysis of the N−O bond, two radicals are generated, but we will focus on the fate of the iminyl radical responsible for the formation of the final product. Our first task was to explore the cyclization of the iminyl radical. We calculated the structures of the iminyl radical resulting from the photocleavage and the six-membered alkyl radical formed after cyclization. These two minima are connected through a transition structure (TS) as shown in Figure 3. In order to fully prove the relevance of the transition structure we also computed the IRC (intrinsic reaction coordinate) connecting these three critical points to confirm that the TS really relates these two minima. As shown in Figure 3, the ring closure must surpass a barrier of ca. 14 kcal/mol through a gradual uphill path at the beginning (which corresponds to a conformational adjustment and no relevant geometry modification) and a progressively steeper incline (corresponding to the radical addition to the alkene). At this point, the key variation is the forming N−C bond. The iminyl radical approaches the alkene moiety reaching the TS point at a distance of 2.095 Å. At the same time, the C═C distance reflects the radical addition with a change in distance from 1.335 Å in **3** to 1.370 Å in the TS while the C═N distance lengthens from 1.251 to 1.262 Å.

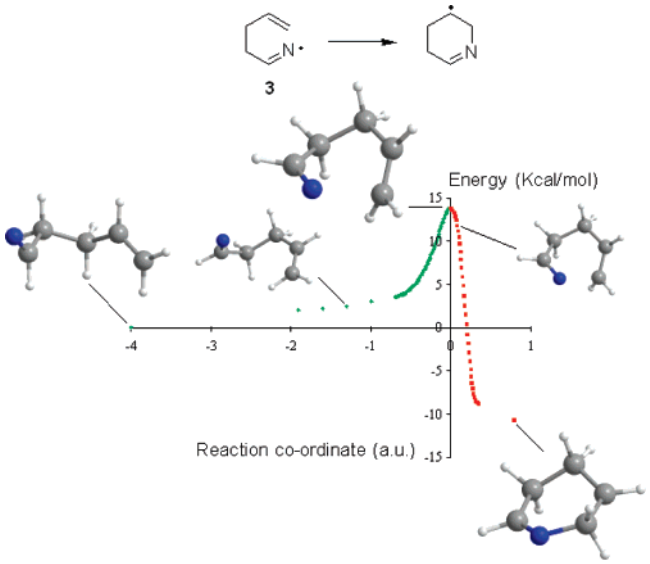

FIGURE 3. S_0 reaction path for the cyclization for radical model **3**.

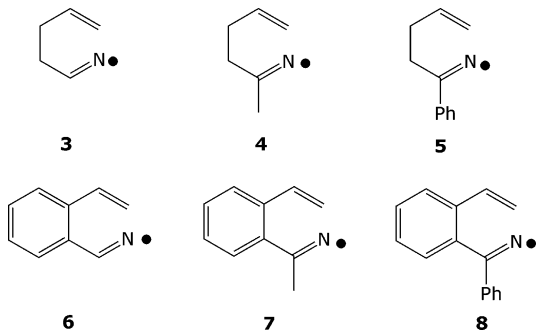

FIGURE 4. Radical models for theoretical calculations.

The next step was to extend the theoretical exploration of the cyclization to several models with different substitution patterns. The compounds considered are shown in Figure 4, and the free energy values for the three critical points for each case are shown in Table 1. Model compounds **4** and **5** are useful to explore the effect of the substituent on the iminic carbon, while compound **6** illustrates the effect of the aromatic ring as a spacer. Models **7** and **8** allow a complete evaluation of the ring closure step as well as a comparison with experimental results.

Computed geometries for the iminyl radicals **3**−**8** share similar parameters. The main difference lies in the relative arrangement of the alkene and imine moieties. While in models **3**−**5** both groups are parallel, in **6**−**8** they tend to be coplanar

(14) Belfield, K. D.; Crivello, J. V. *Photoinitiated Polymerization*; American Chemical Society: Washington, DC 2003.
(15) Lorance, E. D.; Hendrickson, K.; Gould, I. R. *J. Org. Chem.* **2005**, *70*, 2014.
(16) Pinter, B.; DeProft, F.; VanSpeybroeck, V.; Hemelsoet, K.; Waroquier, M.; Chamorro, E.; Veszpremi, T.; Geerlings, P. *J. Org. Chem.* **2007**, *72*, 348.
(17) Pace, A.; Buscemi, S.; Vivona, N.; Silvestri, A.; Barone, G. *J. Org. Chem.* **2006**, *71*, 2740.
(18) Matsubara, H.; Falzon, C. T.; Ryu, I.; Schiesser, C. H. *Org. Biomol. Chem.* **2006**, *4*, 1920.
(19) Arnone, M.; Engels, B. *J. Phys. Chem. A* **2006**, *110*, 12330.

TABLE 1. Free Energies (Δ*G*, kcal/mol) for the Cyclization Step (All Values Are Relative to the Corresponding Iminyl Radical)[a]

compd	TS	alkyl radical
3	16.0	−7.6
4	15.5	−9.1
5	15.3	−10.3
6	5.6	−27.7
7	8.1	−26.7
8	8.1	−25.4

[a] Thermochemical analysis for $T = 298$ K.

SCHEME 2

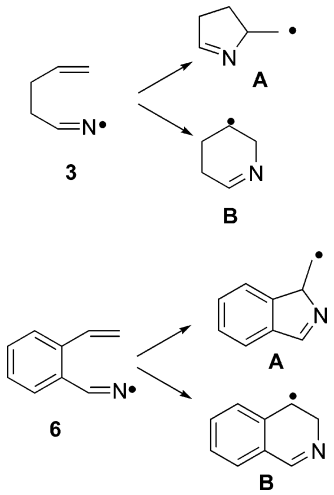

due to the influence of the phenyl group. In the case of the transition state geometries, the relevant parameter is the bond distance of the forming N−C bond. Once again, the difference lies in the presence of the phenyl group as a spacer. While **3**−**5** have N−C bond distances of 2.095, 2.103, and 2.108 Å, respectively, in models **6**−**8**, where the phenyl ring contributes to the radical stabilization, this distance increases to 2.169, 2.179, and 2.175 Å, respectively.

Analysis of the data collected in Table 1 enables some conclusions to be drawn. The transition structures involved in the cyclization step have quite similar geometries, and the energy values depend on the chemical structure. When both the imine and alkene moieties are placed on the aromatic ring (models **6**−**8**), the energy for the transition state is much lower. This can be related to a stabilizing effect of the phenyl group, which contributes by lowering the energy barrier. However, substitution on the iminic carbon has a negligible effect in that both geometries and energies for the two groups (**3**−**5** and **6**−**8**) are very similar. In this case, substitution only becomes important when the substituent is a hydrogen atom, allowing the formation of nitrile and thus lowering the reaction yields through a side reaction.[6]

At this point, we considered the driving force to give five- or six-membered rings, that is to say, the feasibility of the ring closure depending on the position of the radical attack. To clarify this point, we also calculated the cyclization step for **3** and **6** to yield five-membered rings (Scheme 2). The results of these calculations are shown in Table 2. As can be seen, while **6** shows a small preference for the formation of the six-membered ring, model **3** has a preference of more than 3 kcal/mol for the formation of the five-membered ring. In agreement with the calculations on **6**, irradiation of compound **9** yields isoquinoline **10** in 38% yield (Scheme 3).[6] On the other hand, taking into account the calculations on **3**, we believed it to be of interest to test the results in an experimental way. Thus, we prepared acyloxime **11**, which could cyclize at both the five- or six-positions. As shown in Scheme 4, the photoreaction of **11**, in the presence of 1,4-cyclohexadiene to prevent further polymerization, led to the formation of pyrroline **12** in 68% yield, while the six-membered ring isomer was not detected in the crude reaction mixture, a finding consistent with the theoretic prediction. Thus, formation of **A** or **B** (Scheme 2) depends exclusively on the radical precursor. Only one type of product could be experimentally found, although in the case of **6** the calculated energy difference for both processes seems not very high.

TABLE 2. Free Energies for the Cyclization Step to Five- or Six-Membered Rings (All Values Are Relative to the Corresponding Iminyl Radical)

compd	TS-A	TS-B	product A	product B
3	12.6	16.0	−5.2	−7.6
6	6.4	5.6	−10.6	−27.7

SCHEME 3

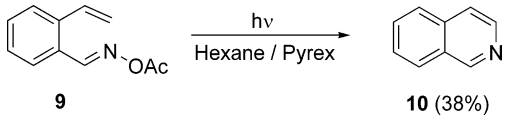

SCHEME 4

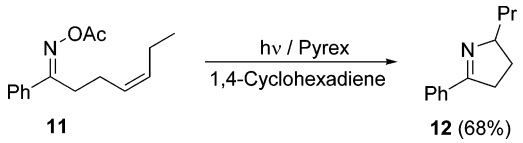

TABLE 3. Irradiation of 11 in the Presence of Different Triplet Quenchers and Sensitizers

entry	ketone	E_T[a] (kcal/mol)	**12**/**11** ratio[b]
1	benzophenone	69	3.93
2	2-acetylnaphthalene	59	1.88
3	1-acetylnaphthalene	56	0.14
4	none		0
5	9-fluorenone	50	0

[a] See ref 21. [b] Irradiation was carried out for 2 h

Photochemical Aspects. Since the understanding of a photochemical reaction requires knowledge of the processes occurring at the molecular level from the absorptive act to the formation of products, we report in this section results of the standard studies such as excited-state quenching, quantum yield, excited-state sensitizers, laser flash photolysis experiments, the Stern−Volmer plot, and luminescence measurements.

Taking into account that the formation of pyrroline derivatives from iminyl radicals is a more general procedure, we decided to study the cyclization of acyloxime **11**. The nature of the excited-state involved in this process was first investigated by carrying out the irradiation in the presence and in the absence of molecular oxygen, which is an effective triplet state quencher for a large number of photoreactions. Since we confirmed that O_2 slows the reaction down, we assessed the effect of different triplet state quenchers and sensitizers on the irradiation of this acyloxime. Compound **11** does not absorb above 330 nm and, therefore, its irradiation was carried out through a solution filter

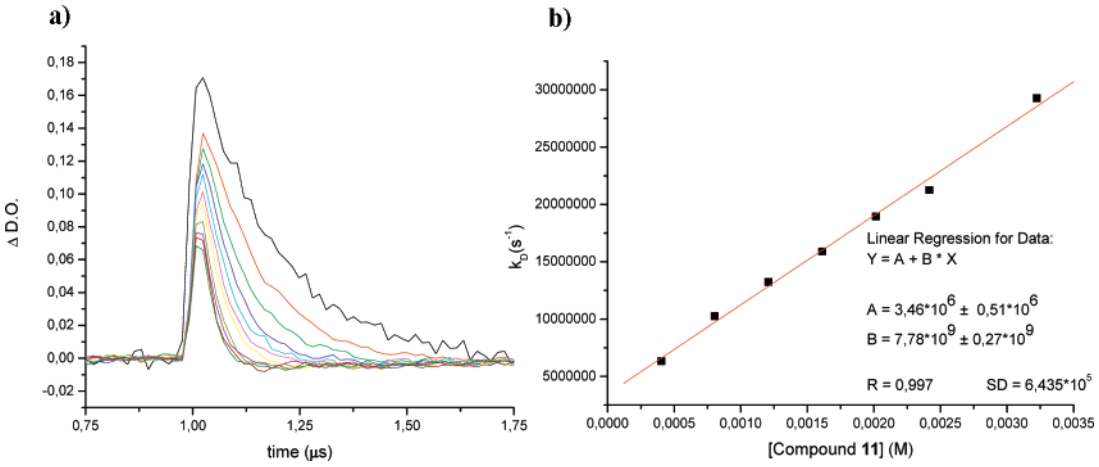

FIGURE 5. (a) Triplet-state decay plots of a solution of xanthone in acetonitrile with different amounts of **11**. (b) τ inverses (k_D) versus the amount of *O*-acetyloxime added.

that removed λ radiation under 330 nm.[20] The data for the reaction of acyloxime **11** (1×10^{-2} M), to give the 1-pyrroline **12**, in the presence of different ketones in deoxygenated acetonitrile are summarized in Table 3. Ketones can act as triplet state sensitizers or quenchers depending on their relative energies compared with that of **11**. We used ketones in the range 79−50 kcal/mol.[21] The reaction gave **12** with benzophenone, 2-acetylnaphthalene or 1-acetylnaphthalene but not with 9-fluorenone. These results indicate that the reaction takes place under triplet state conditions. The triplet state energy of **11** was estimated to be between 56 and 50 kcal/mol.

The triplet state was also studied by laser flash photolysis. The triplet state decay of a 4.03×10^{-4} M solution of xanthone in acetonitrile was measured. Subsequently, 1, 2, 3, 4, 5, 6, and 8 equiv of **11** were added as a quencher, and the decay plots were recorded.

All graphs were fitted with exponential functions in order to find the xanthone life time, τ, for each experiment. The τ inverses (disappearance constants, k_D) were then plotted versus the amount of *O*-acetyloxime added. The straight line obtained shows compound **11** to be a triplet quencher (Figure 5). The quenching rate, $k_D = 7.8 \times 10^9$, is obtained from the linear fit slope. This value is typical of diffusional quenching.

We proceeded to investigate the quenching of the photoreactivity of **11**. We chose the common triplet-state quencher 2,5-dimethyl-2,4-hexadiene, since it possesses an appropriate triplet energy (42 kcal/mol)[22] and does not show any absorption at the irradiation wavelengths (solution filter, $\lambda > 330$ nm). The plot of quantum yield of disappearance of **11** (ϕ^0/ϕ, where the superscript zero denotes the absence of quencher) versus concentration of 2,5-dimethyl-2,4-hexadiene (see Figure 6 a) is typical for a situation in which two excited states (singlet and triplet) undergo the same reaction and only one of them is selectively quenched.[23] Extrapolation of the plateau to the ϕ^0/ϕ coordinate yields 0.24. Assuming that this unquenchable reaction is due to the reaction of **11** from the singlet state, the contribution

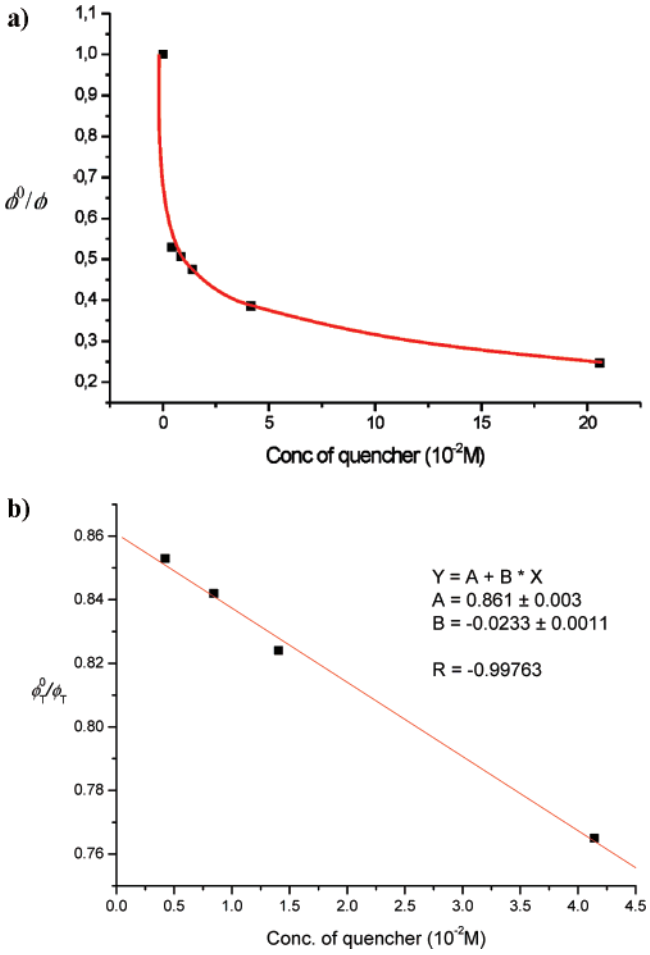

FIGURE 6. (a) Experimental plot of quantum yield rate of disappearance of **11** versus concentration of 2,5-dimethyl-2,4-hexadiene for the irradiation of **11**. (b) Stern−Volmer plot for the reaction of *O*-acyloxime **11** after subtracting singlet contribution.

of the triplet state reaction to the slope may be determined by subtracting 0.24 from the experimental values of ϕ^0/ϕ. Thus, a normal Stern−Volmer plot results with an intercept of 0.86 ± 0.01 and a slope of $k_q\tau = -2.3 \pm 0.1$ M^{-1}, where k_q is the quenching rate constant, for the triplet reaction alone (Figure 6b).

(20) Concentrations: $NaBr \cdot 2H_2O$, 650 g/L; $Pb(NO_3)_2$, 3 g/L. See, for example: *CRC Handbook of Organic Photochemistry*; Scaiano, J. C., Eds.; CRC Press: Boca Raton, 1989; Vol. I, p 48.

(21) Murov, S. L.; Carmichael, I.; Hug, G. L. *Handbook of Photochemistry*, 2nd ed.; New York, 1993; p 54.

(22) See ref 21, p 60.

(23) Turro, N. J. *Modern Molecular Photochemistry*; University Science Books: Sausalito, CA, 1991; p 253.

TABLE 4. Emission Data for a Solution of 11 in Methylene Chloride

T (K)	λ_{exc} (nm)	λ_{em} (nm)	τ (s)
298	309	380	10.6
77	300	350	10.8

Next, we studied the emission properties of compound **11**. Emission data for a solution 0.16 M in CH_2Cl_2 of this compound are shown in Table 4. *O*-Acyloxime **11** shows an emissive state at both room temperature and 77 K. These long emission lifetimes ($\tau = 10.6-10.8\ \mu$s) are suggestive of triplet parentage. These lifetime values are in agreement with those found in literature for *O*-acyloximes triplet states.[24] From the triplet lifetime at 298 K and the Stern−Volmer plot slope, $k_q\tau$, a quenching rate constant, k_q, value of ca. $2.2 \times 10^5\ M^{-1}\ s^{-1}$ is calculated.

Consistent with the calculated MEP energy profile, where relaxation on the S_2 PES leads directly to N−O bond cleavage (see Figure 2), no fluorescence was detected in those experiments.

Finally, we also determined the quantum yield of the efficiency of appearance of **12** from the photoreaction of **11**. *trans*-Azobenzene was used as an actinometer,[25] and the irradiation was performed at 313 nm using a monochromator. The quantum yield for the formation of **12** for a 0.107 M solution of **11** in deoxygenated acetonitrile was found to be $\Phi_R = 0.05 \pm 0.01$.

Conclusions

We have investigated the photochemically induced iminyl radical cyclization reactions of acyloximes. Theoretical calculations (CASPT2/6-31G*//CASSCF/6-31G* level, using an active space of 14 electrons in 11 orbitals) indicate that S_2 should be the spectroscopic state and its relaxation leads directly to N−O bond breaking, due to the coupling between the imine π^* and the σ^* N−O orbitals, with the formation of iminyl radicals. Our calculations, carried out at the B3PW91/6-31+G* level, suggest that iminyl radicals could evolve through cyclization to the six- or five-membered ring, depending on the presence or absence of a phenyl group as a spacer. This fact has been experimentally verified by irradiation of 2-vinylbenzaldehyde *O*-acetyloxime and (*Z*)-1-phenyl-4-hepten-1-one *O*-acetyloxime, respectively. The photochemical aspects, such as excited-state quenching, quantum yield, excited-state sensitizers, laser flash photolysis experiments, and Stern−Volmer plot, of the more common five-membered ring formation were investigated. These studies reveal that singlet and triplet excited states undergo the same reaction. Emission lifetimes of ca. $\tau = 10.6\ \mu$s for compound **11** are suggestive of triplet parentage, while no fluorescence was detected, in agreement with the computed MEP energy profile.

(24) Bucher, G.; Scaiano, J. C.; Sinta, R.; Barclay, G.; Cameron, J. *J. Am. Chem. Soc.* **1995**, *117*, 3848.

(25) Kuhn, H. J.; Braslavsky, S. E.; Schmidt, R. *Pure Appl. Chem.* **2004**, *76*, 2105.

Experimental Section

General Procedure for Irradiation. The acyloxime **11** (0.5 mmol) and 10 equiv of 1,4-ciclohexadiene (5 mmol) were dissolved in 50 mL of deoxygenated acetonitrile and irradiated at room temperature under an Ar atmosphere through Pyrex glass with a 400 W medium pressure-mercury lamp until the oxime was consumed (TLC, hexane/AcOEt, 4:1). The solvent was then removed with a rotary evaporator, and the products were separated by chromatography (silica gel, hexane/AcOEt).

5-Phenyl-2-propyl-3,4-dihydro-2*H*-pyrrole (12): colorless oil; yield 64 mg, 68%; ^{1}H NMR (300 MHz, $CDCl_3$) δ 7.85 (dd, J = 3.0, 3.0 Hz, 2H), 7.44−7.36 (m, 3H), 4.28−4.12 (m, 1H), 3.01−2.95 (m, 1H), 2.93−2.84 (m, 1H), 2.27−2.12 (m, 1H), 1.89−1.76 (m, 1H), 1.67−1.55 (m, 1H), 1.55−1.40 (m, 3H), 1.02−0.94 (t, J = 6.0 Hz, 3H); ^{13}C NMR (300 MHz, $CDCl_3$) δ 171.83, 134.94, 130.32, 128.48, 127.75, 73.21, 39.08, 35.06, 28.69, 20.05, 14.41; ES (+) m/z 188 (M + 1). Anal. Calcd for $C_{13}H_{17}N$: C, 83.37; H, 9.15; N, 7.48. Found: C, 83.42; H, 9.13; N, 7.45.

Acknowledgment. We thank the Spanish MEC (CTQ2007-64197) and the Comunidad Autónoma de La Rioja (ACPI2005/06) for financial support. D.S. is financed by the Ramón y Cajal program from the MEC. R.A. thanks the Comunidad Autónoma de La Rioja for his fellowship.

Supporting Information Available: Experimental procedures, characterization data for new compounds, and Cartesian coordinates for the calculated geometries. This material is available free of charge via the Internet at http://pubs.acs.org.

JO7025542